Functionalization of Frustules of the Diatom *Staurosirella pinnata* for Nickel (Ni) Adsorption From Contaminated Aqueous Solutions

Saverio Savio [1,2†], Serena Farrotti [1,3†], Andrea Di Giulio [4,5], Serena De Santis [6], Neil Thomas William Ellwood [4], Simona Ceschin [4] and Roberta Congestri [1]*

[1] Laboratory of Biology of Algae, Department of Biology, University of Rome 'Tor Vergata', Rome, Italy, [2] PhD Program in Evolutionary Biology and Ecology, University of Rome 'Tor Vergata', Rome, Italy, [3] AlgaRes S.r.l., Via Antonio Silvani 130, Rome, Italy, [4] Department of Science, Roma Tre University, Rome, Italy, [5] Interdepartmental Laboratory of Electronic Microscopy (LIME), Roma Tre University, Rome, Italy, [6] Department of Industrial, Electronic and Mechanical Engineering, Roma Tre University, Rome, Italy

The structural characteristics of diatom cell walls (frustules) has led to their widespread use in diverse biotechnological applications, some of which can be further improved by surface chemical modification (functionalization). The use of coating agents can significantly increase surface binding capacity for target compounds. Frustules of the diatom *Staurosirella pinnata* used here were a by-product after applying a cascade-extraction process (for other products) to mass cultures. The protocol for the cleaning and functionalization of raw frustules using 3-Mercaptopropyl-trimethoxysilane and 3-Aminopropyl-trimethoxysilane was optimized and reported. Functionalization efficacy was observed using Electron Microscopy, Energy Dispersive X-ray Spectroscopy and Fourier-Transform Infrared Spectroscopy. Optimally functionalized frustules were evaluated for nickel removal from aqueous solutions. Incubations of 10 min, using 1 g/L of frustules, gave almost complete Ni removal with functionalized frustules compared to 3% removal by raw frustules. The proposed protocol represents a reproducible and efficient alternative for Ni removal from contaminated water.

Keywords: diatom frustules, diatom biotechnology, diatom biomass, heavy metal removal, nanoporous silica, functionalization

INTRODUCTION

Diatoms are an abundant and widespread group of unicellular, aquatic, microalgae that produce an external silicified cell wall, the frustule, made up of different parts (valves and girdle bands). Frustule morphological features are highly elaborated and species specific. Valves and bands bear ordered, hierarchical patterns of micro- and nano- pores that are inherited through generations, *via* a strong genetically controlled deposition process (Heintze et al., 2020). Frustules confer adaptive advantages to diatoms, such as mechanical resistance against grazers, hydrodynamic stress and buoyancy-control (Hamm et al., 2003; De Stefano et al., 2009; Arrieta et al., 2020). In addition, the quasi-periodic and highly regular diatom pore patterns showed interaction with light, providing protection against harmful radiation and optimization of incident light for photosynthesis

(Di Caprio et al., 2014; Ferrara et al., 2014; De Tommasi et al., 2018). Frustule architecture also produces an efficient interface area and surface area:volume ratio enhancing the cell-environment exchanges (Mitchell et al., 2013).

The combination of adaptability to changes in environmental conditions and high growth rates has led to a recent advancement in the knowledge of intensive diatom cultivation for biotechnology purposes. This advancement takes advantage of both cellular biochemistry and frustule porous characteristics (aquafeed field, nutraceutics and pharmaceutics, nanotechnology and biomimetics) (Lamastra et al., 2014; Gilbert-López et al., 2017; Kiran Marella et al., 2020; Savio et al., 2021). Technological exploitation of the nanoporous structure of frustules has been further advanced by methods that modify frustules while maintaining its hierarchical structures. Chemical modification of frustule surfaces by functionalization using coating reagents such as amino- and mercapto-silanes (Novelli et al., 2017; Gutiérrez Moreno et al., 2020) improves their binding capacity for certain target compounds. This type of functionalization has been used for drug carriers (Rea et al., 2014; Terracciano et al., 2015), optical sensors (Selvaraj et al., 2018) and adsorbents for frustule application in water treatment, ion exchange and filtration (Khraisheh et al., 2004). Water contaminated with heavy metals is a wide-spread health concern, even when present in trace amounts due to their chronic accumulation in organs over time (Ali et al., 2019). Nickel, for example, is one of the most toxic pollutants, and the by-product of its energy intensive production is the generation of large amounts of solid wastes that require proper handling and valorization to avoid risks to environmental and human health. Nickel consumption is associated with a wide range of acute or chronic health conditions, including epidermal allergic reactions, cardiovascular and kidney diseases, lung fibrosis and lung and nasal cancers. In addition, nickel is able to cross the placenta and alter maternal hormonal balances and can therefore affect the fetus both directly and indirectly (Cempel and Nikel, 2006). When compared to food, water represents a minor proportion of daily exposure to nickel (WHO, 2005), however, the absorption of soluble nickel compounds from drinking-water is significantly higher than that from food (Solomons et al., 1982). Observations of the chemical status of Italian inland waters under the Water Framework Directive have shown that between 10 to 30% of surface waters (20 to 40% still unknown) and 30 to 60% of groundwaters have not gained good status (WISE, 2018). Of the 562 tons of chemical substances released into Italian water bodies annually, around 80% are shown to be heavy metals (Legambiente, 2020). Heavy metals are therefore considered as priority pollutants and are monitored closely by the controlling agencies in attempts to adhere to the 20 mg L^{-1} limit for drinking waters under the Water Framework Directive (Directive 2000/60/EC). The most common and conventional approaches to remove heavy metals from waters utilise activated carbon, clay minerals, zeolites or polymers (Zhao et al., 2019). Due to the scale of the heavy metal problem, the development of effective and inexpensive adsorbents is an active area of research. Abundant and inexpensive fossilized frustules (diatomite) have been previously used, but their real potential as adsorbent is hampered by some intrinsic features. Diatomite is a highly variable material, containing many impurities, like terrigenous particles and inorganic oxides; it is also highly heterogeneous, as type, shape, size and fragmentation of the frustules result in unpredictable behaviour (Danil de Namor et al., 2012; Lamastra et al., 2014; Uthappa et al., 2018).

To overcome the problems associated with diatomite, frustules can be obtained from extant diatoms, especially when cultivated in monospecific cultures. Cultured diatoms can be considered as *nano-factories*, able to produce up to 10^6 frustules per mL (Wang and Seibert, 2017) which would be structurally identical with overall more predictable functions (Rogato and De Tommasi, 2020). In addition, biorefinery of diatoms would result in biomass from which different bioproducts could be extracted beforehand (Gilbert-López et al., 2017; Savio et al., 2020). The exhausted biomass at the end of cascade extractions, would be constituted by frustules ready for functionalization, improving the overall value of the biomass and the sustainability of the process.

The aim of this study, was to optimize the functionalization of frustules of the diatom *Staurosirella pinnata* (Ehrenberg) D.M.Williams & Round, obtained from the exhausted biomass of a diatom culture biorefinery (De Angelis et al., 2016; Savio et al., 2020) and to use them in the treatment of a wastewater contaminated with nickel. The main functionalization protocol parameters will be adjusted to best preserve the frustule porous ultrastructure and morphology whilst giving a homogeneous silane coating. Then functionalized frustules will be compared to raw (unfunctionalized) frustules for their capacity to remove nickel from aqueous solutions, prospecting their potential as a novel and efficient adsorbent.

MATERIALS AND METHODS

Frustule Preparation

Staurosirella pinnata was intensively cultivated on ten occasions in an indoor, column-photobioreactor (8L), and then harvested at the stationary phase. Clean frustules of *S. pinnata* were obtained from biomass remaining after cascade extractions for other potentially valuable co-products (Savio et al., 2020). Briefly, the pooled biomass was lyophilized, manually grinded and then extracted with a solution of milli-Q water and MetOH (20% v/v) for 2 hours at 45°C to obtain a crude extract. Subsequently, the residual biomass was treated with CHCl$_3$ and MetOH (2:1 v/v) following the method of Bligh and Dyer (1978) to extract total lipids and, finally, the "leftover" material (exhausted biomass), was treated with acid solutions to remove any organic residues and to give clean frustules. Three different cleaning protocols were tested, one based on H$_2$SO$_4$:HNO$_3$:H$_2$O (3:1:1 v/v/v) at 90°C for 2 h, another on HNO$_3$:H$_2$SO$_4$ (2:1 v/v) at 90°C for 2 h, and the last using H$_2$SO$_4$:HNO$_3$ (3:1 v/v) at 90°C for 1 h. Samples were then centrifuged (3000 x *g* for 5 min); the supernatants were discarded and the pellets were washed repeatedly with milli-Q water until pH neutrality was reached. Finally, cleaned frustules

were lyophilized (hereafter referred to as raw frustules) and preserved at -20°C for Scanning Electron Microscopy analysis (SEM) and surface functionalization.

Frustule Surface Functionalization

Development of the surface functionalization of the raw frustules was carried out using an *ad hoc* protocol in order to obtain a homogenous coating while preserving their porous ultrastructure.

Following the protocol of Zhang et al. (2015), lyophilized frustules (0.2 g) were resuspended in milli-Q water (20 mL) and hydroxylated with NH_4OH (1 mL, 30%). Subsequently, the material was functionalized using two silanizing agents: 3-Aminopropyl-trimethoxysilane (APTMS, 1 mL, molecular weight: 179.29) and 3-Mercaptopropyl-trimethoxysilane (MPTMS, 1 mL, molecular weight: 196.34) to incorporate primary amine ($-NH_2$) and thiol ($-SH$) groups on frustule surfaces. After each adjustment of the functionalization protocol the frustules were observed using SEM, to determine the dispersal and ultrastructural properties of the frustules and the any absence of APTMS and MPTMS aggregates. First modifications of the protocol involved changing solvents to improve the coating process, to better preserve frustule ultrastructural features and to reduce the amount of silane aggregates. In place of milli-Q water, two nonpolar solvents were evaluated, the commonly used toluene and the lowly-toxic and non-carcinogenic, hexane. Further, different functionalization parameters were modified to regulate silane coating: i) concentration of the hydroxylation reagent NH_4OH, (4, 5, 10, 20, 30 and 40 mM); ii) concentration of the functionalization reagents APTMS/MPTMS (1:1 v/v, 7 mM and 14 mM) and iii) time of the functionalization reaction (1, 3, 5, 9 and 18 h).

The obtained functionalized frustules were washed with ethanol, dried at 40°C and stored at -20°C.

Structural and Surface Analysis of Functionalized Raw Frustules

Preparation of functionalized frustules for SEM observations involved resuspending dried material in absolute hexane, suspensions (5 μL) were then dispersed over aluminium stubs and air dried in a fume hood. The dried material was examined using a Gemini 300 field emission microscope at a voltage of 5 kV (Carl Zeiss AG, Jena, Germany), equipped with an XFlash 6-60 Energy Dispersive X-Ray Spectroscopy (EDS) system (Bruker Nano GmbH, Berlin, Germany). EDS analyses were performed to determine the elemental composition of the samples at 10 kV accelerating voltage, secondary detector and working distance 7.5 mm. Before SEM sessions, samples were gold coated for avoiding charging effects by using Emitech K550 unit and Quorum-SC7620 sputter instrument.

Fourier-Transformed InfraRed (FTIR) spectra of samples were also collected in the $4000 - 650$ cm^{-1} regions using a Nicolet iN10 infrared microscope (Thermo Fisher Scientific IT, Milano, Italy) equipped with a Mercury-Cadmium-Telluride (MCT-A) nitrogen-cooled detector in reflection mode. Sixty-four interferograms were averaged per spectrum; nominal spectral resolution was 4 cm^{-1}. Data acquisition and spectra elaboration were carried out with the OMNIC SPECTA software provided by Thermo Fisher Scientific.

Nickel Adsorption Tests of Functionalized Raw Frustules

Nickel adsorption capacity of raw material and functionalized frustules was evaluated in a preliminary test using an adsorbent concentration of 1.0 g/L in milli-Q water (20 mL) containing Ni (1.10 mg/L). Samples incubation was carried out at three pH values (4.0, 7.0 and 10.0) for 24 h. A second test was then carried out to evaluate the removal efficiency of both frustule types as a function of time, using Ni (30 mg/L) and collecting samples at discrete times following the start of the incubation (10, 30, 60 min and 5 h). Each test was carried out in triplicate in conical tubes shaken (15 mL) shaken (200 rpm) on an orbital shaker (IKA® KS 130). All experiments were carried out at room temperature (25°C). To terminate the incubations, the samples were centrifuged at 3000 x g and the supernatants collected for determination of Ni concentration, the pellets were analysed using FTIR.

The concentration of nickel was determined spectrophotometrically at 560 nm using the 1-(2 pyridylazo)-2-napthol (PAN) method. Deionized water was used as a blank and standard curves prepared from 5 to 0.1 mgL^{-1} using a standard Ni solution (1000 mg/L $Ni(NO_3)_2$, NIST).

Data Analysis

GraphPad Prism version 9.0 program (GraphPad Software, San Diego, CA, USA) was used for statistical analysis. Two-Way ANOVA and Tukey's HSD test were performed (a p-value of <0.05 was considered statistically significant) and, for each treatment, standard deviations (SD) were calculated and reported.

RESULTS AND DISCUSSION

Cleaning Protocol Selection and Raw Frustule Characterization

All frustules observed using SEM, irrespective of the cleaning protocol, showed morphological and ultrastructural features typical of the species as described from cultured (De Angelis et al., 2016) and natural material (Haworth, 2007). Valves were almost round in shape and beared bilateral rows of circular pores (average diameter of 5.23 μm ± 0.73 μm), internally occluded, separated by a hyaline, unperforated central area. The valve margine presented spines as triangular projections that link adjacent sibling cells together. This indicates that the mass cultivation and the sequential extractions performed on the biomass of *S. pinnata* did not significantly alter the morphology of frustule valves and pores.

All three cleaning protocols removed residual organic matter in the samples and no inorganic debris (mostly crystallized culture medium) was found (**Figure 1**). Although cleaning treatments in general did not significantly alter frustule morphology, a higher degree of valve and girdle fragmentation was evident in the treatments using $H_2SO_4:HNO_3:H_2O$ 3:1:1 (**Figure 1A**) and $HNO_3:H_2SO_4$ (**Figure 1B**). The best valve integrity and organic matter removal were observed in samples cleaned using $H_2SO_4:HNO_3$ 3:1; under this treatment there was also minimal detachment of girdle bands (**Figure 1C**).
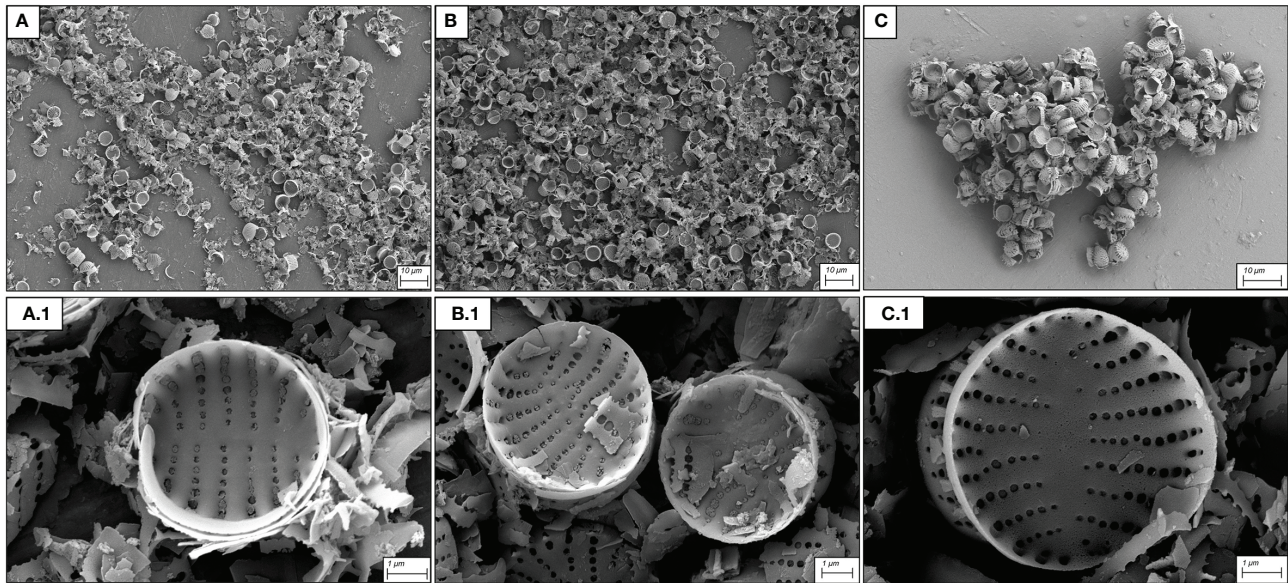
FIGURE 1 | SEM micrographs of *S. pinnata* valves obtained with different hot acid cleaning protocols. **(A)** H_2SO_4:HNO_3:H_2O (3:1:1 v/v/v) at 90°C for 2 h; **(B)**: HNO_3:H_2SO_4 (2:1 v/v) at 90°C for 2 h; **(C)**: H_2SO_4:HNO_3 (3:1 v/v) at 90°C for 1 h. **(A1–C1)** represent details at higher magnification of **(A–C)** respectively.

Frustule Surface Functionalization and Protocol Development

During functionalization, solvent choice has been shown to be an important factor to maintain the underlying morphology of silicon surfaces and, thus, the adsorption capacity (Jakša et al., 2014). The effect of different solvents in 18 h functionalization experiments is shown in the SEM micrographs (**Figure 2**). The use of milli-Q water as a solvent caused a high number of aggregates due to the uncontrolled aggregation of APTMS with MPTMS and frustules (**Figures 2A, D**) that appeared incorporated and overcoated by silanes. Following the protocol proposed by Zhang et al. (2015) there was a loss of the frustule
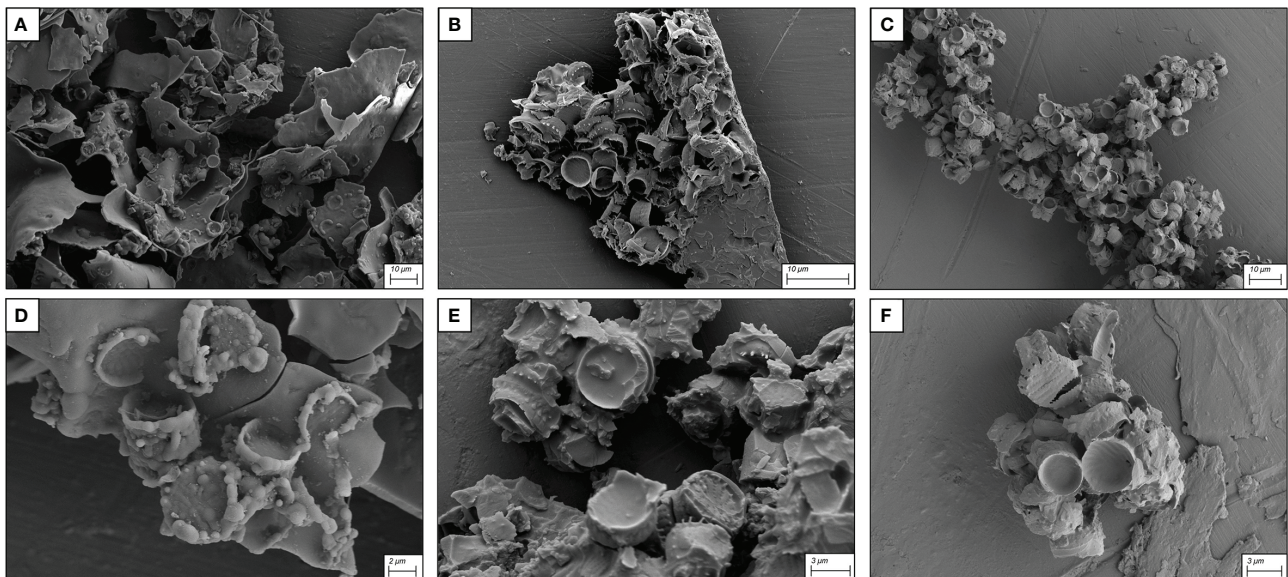

FIGURE 2 | SEM micrographs of frustules functionalized with the three solvents: **(A)**: milli-Q water, **(B)**: toluene and **(C)**: hexane. **(D–F)** show details at high magnification of the same solvent conditions as **(A–C)** respectively.

ultrastructural properties due to excessive overlaying of silanizing agents, which significantly altered the available surface area for Ni binding. This type of surface simplification and the coagulation of frustules significantly reduces the overall porosity and the adsorption capacity of the frustules, which will diminish their biotechnological potential in several applications (Anedda et al., 2003; González-Fortuna et al., 2021). Toluene- (**Figures 2B, E**) and hexane-functionalized frustules (**Figures 2C, F**) greatly reduced the over-presence of silane precipitates and frustule aggregation and gave a more even coating compared to the samples functionalized in milli-Q water. However, on closer observation, the less toxic solvent hexane gave the best performance in terms of the coating homogeneity and was therefore used in the subsequent experiments.

To optimize the homogeneity of coating, different functionalization times (1, 5, 9 and 18 h) were also evaluated. Analysis of SEM micrographs showed no time effect on surface modification by APTMS and MPTMS, indicating that this parameter did not influence coating homogeneity.

Hydroxylation of surfaces is an important requirement in the functionalization process, because silane deposition is strongly influenced by availability of hydroxyl groups that are the binding sites for silane linkers (Parikh et al., 2002; Arranz et al., 2008; Ogata et al., 2009; Mack et al., 2017). Therefore, the tests performed over 9 h with decreasing hydroxylation reagent

(NH_4OH) concentrations (30, 20, 10 and 5 mM) were expected to reduce over-coating and frustule coagulation and preserve frustule morphology.

At NH_4OH concentrations of about one order of magnitude lower than that proposed by Zhang et al. (2015) (30 mM, **Figure 3A** and 20 mM, **Figure 3B**) there were still over-deposition of silanes on frustules, reduction of the porous pattern and presence of large frustule aggregates. At the lower NH_4OH concentrations (10 mM and 5 mM), the homogeneity of the silane coating was improved with the original morphology and ultrastructural features mostly preserved (**Figures 3C, D**)

To further refine functionalization, on the basis of the aforementioned results, two protocols were selected and tested, i) 2.5 mM of NH_4OH, 14 mM of APTMS and 14 mM μL of MPTMS for 9 h of functionalization, hereafter referred to as *Protocol 1* (**Figure 4A**) and ii) 2 mM of NH_4OH, 7 mM of APTMS and 7 mM of MPTMS for 18 h of functionalization, hereafter referred to as *Protocol 2* (**Figure 4B**).

The SEM micrographs (**Figures 4A, B**) clearly showed that samples treated with the two protocols exhibit a homogenous coating of surfaces by silanes, with negligible differences. Both protocols resulted in a coating that preserved the frustule ultrastructural properties, with nanopores not obstructed by an excess of silane linkers.
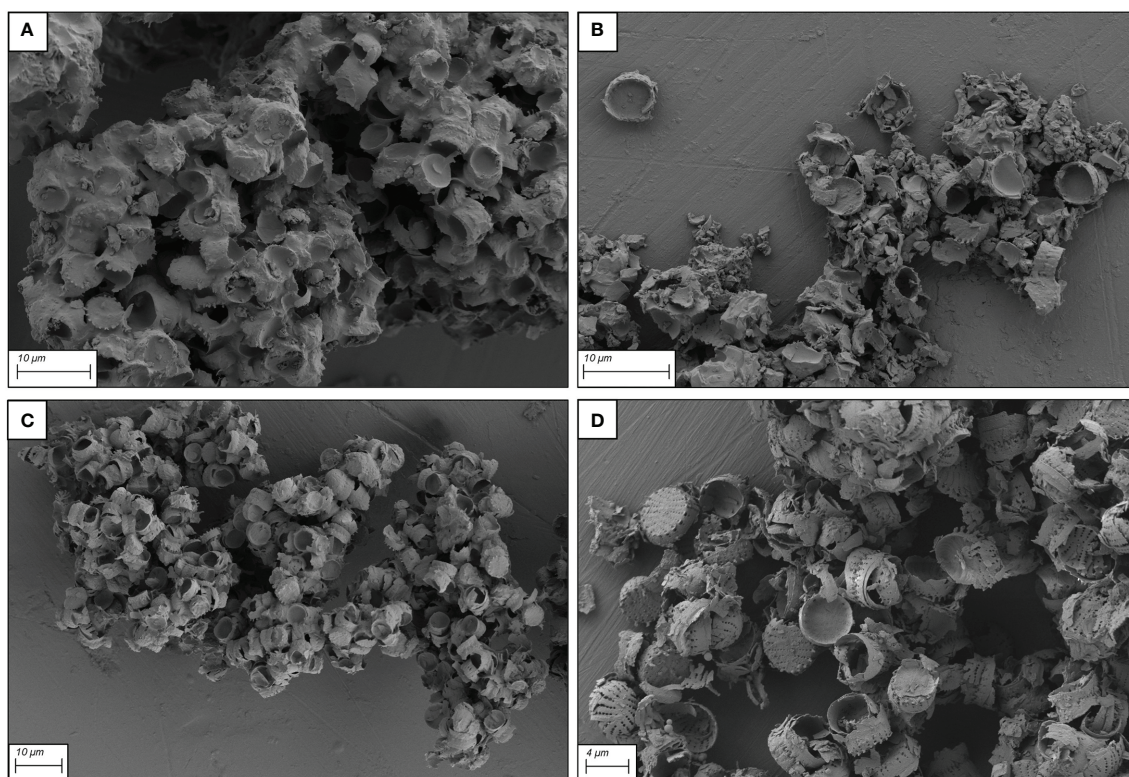

FIGURE 3 | SEM micrographs of functionalized frustules after 9 h functionalization with different concentrations of the hydroxylation reagent NH_4OH. **(A)** 30 mM, **(B)** 20 mM, **(C)**: 10 mM and **(D)**: 5 mM.
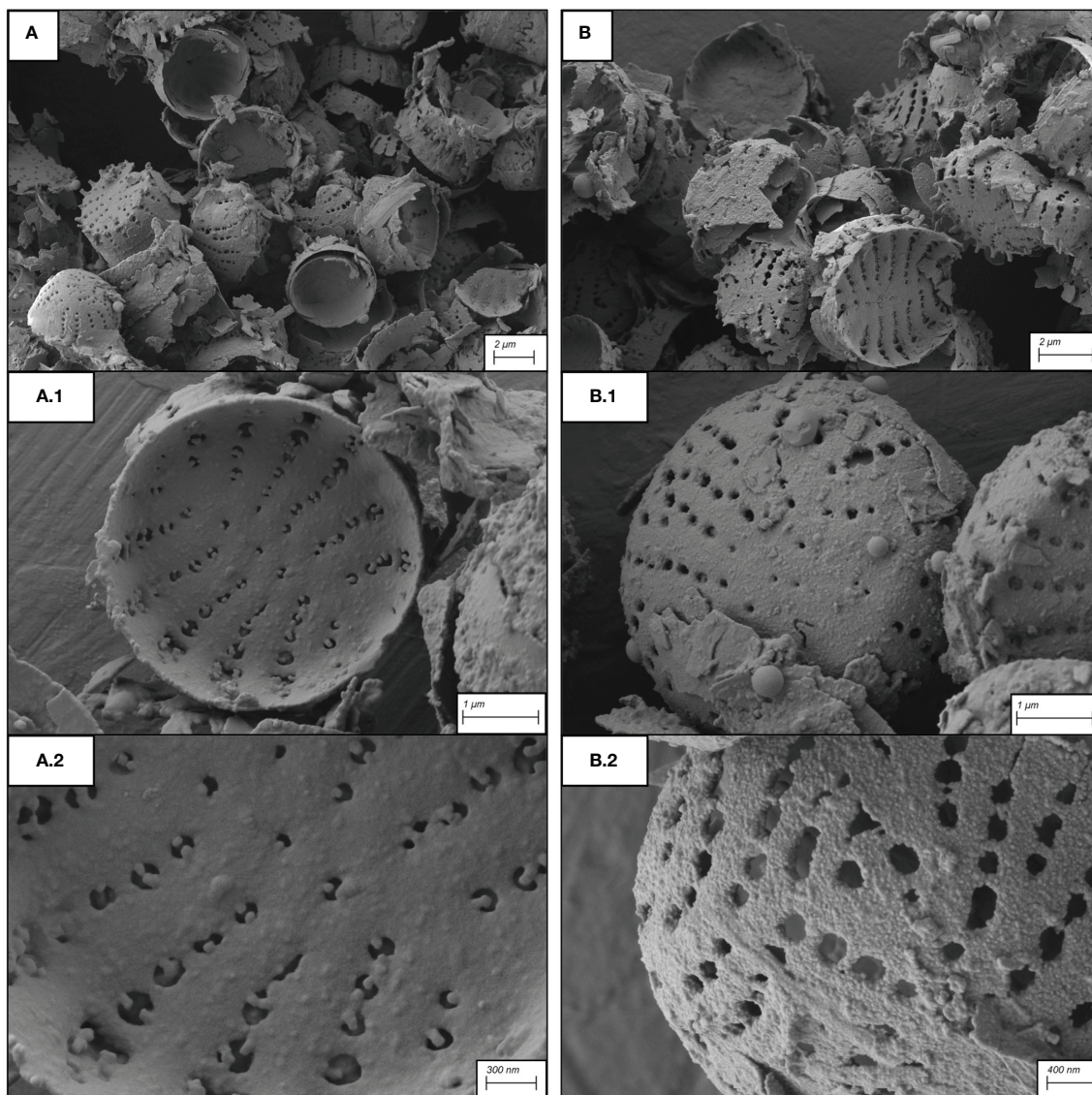
FIGURE 4 | SEM micrographs of frustules after application of the two protocols. **(A)**: *Protocol 1*; **(B)**: *Protocol 2.* **(A1, A2, B1, B2)** represent high magnification of A and B respectively.

Functionalized and Raw Frustule Surface Characterization

To ascertain the successful incorporation of thiol and amino groups onto the diatom frustule surfaces, Energy Dispersive X-ray Spectroscopy (EDS) analysis was also performed (**Figure 5**).

The EDS spectra of the functionalized frustules clearly demonstrated the presence of nitrogen and sulphur which are not present in the raw frustules. This clearly indicates the addition of thiol and amino groups onto the frustule surfaces from the functionalizing coating of APTMS and MPTMS. It is also likely that the increase in carbon in the functionalized frustules is associated with the polymer coating.

As a further demonstration, FTIR spectra were obtained for the functionalized and raw frustules (**Figure 6**).

The weak -SH signal expected at about 2750 cm^{-1} is not clearly visible on the spectra of treated sample, but the -CH band at 2928 cm^{-1}, due to the symmetric CH_2 stretching vibration, and the -NH_2 signal at 1562 cm^{-1}, suggest the successful grafting of APTMS and MPTMS onto the diatom silica surface and, thus, the incorporation of amino and thiol groups.

Ni Adsorbance Capacity of Raw and Functionalized Frustules

The adsorbance capacity of functionalized frustules was analyzed in a preliminary adsorption test (24 h) using an artificial contaminated water with Ni concentration of 1.10 mg/L under three pH values (4.0, 7.0 and 10.0) (**Figure 7**).
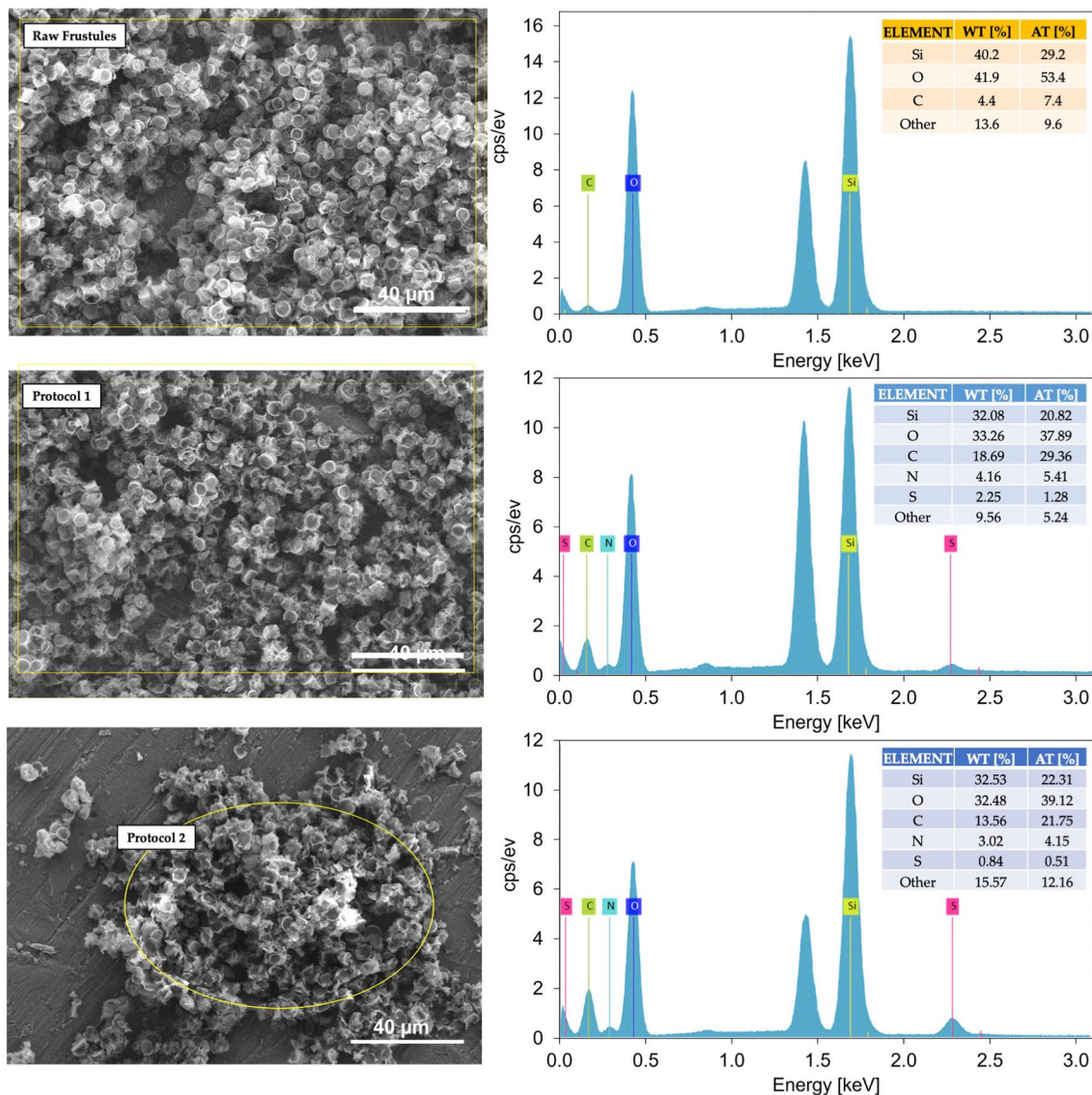
FIGURE 5 | Representative SEM-EDS spectra of raw and functionalized frustules using *Protocol 1* and *Protocol 2*. At 1.5 keV the aluminium signal arising from the support used for samples deposition appears.

The Ni adsorption of the functionalized frustules did not show any pH dependence, with a removal efficiency of around 94% under all pH conditions (**Figure 7**). On the other hand, the Ni adsorption of the raw frustules increased with pH, but only up to 38% Ni removal from solution at pH 10.0. Ni removal by raw frustules can be ascribed to the presence of free hydroxyl groups on their surface which can serve as binding sites for metal ions (Townley, 2011). The binding interaction is strongly dependent from pH that affects the frustule degree of ionization and surface charge (Tozak et al., 2013).

The data of the functionalized frustules contrasted with previous findings for functionalized diatomite, diatom silica microparticles and a wide range of functionalized nanocomposites, that, despite the promising heavy metal removal efficiencies, showed a strong pH dependency (Zhang et al., 2015; Wu et al., 2021). For example, magnetic chitosan nanoparticle appears as an efficient and fast tool for removing Pb^{2+} from water, with an efficiency close to 100% at acid and neutral pH conditions (Liu et al., 2009), but increasing pH up to 7.0 seemed to affect the lead ion binding by chitosan, thus decreasing its adsorption capacity. Similarly, functionalized diatom microparticles are able to remove mercury from water with a maximum removal efficiency at pH 6, however, at pH <5.0, the interactions of the functional groups with Hg(II) decrease, evidencing that pH plays an important role in the adsorption mechanism (Yu et al., 2012). If Ni adsorption by functionalized frustules is not pH dependent as shown in our work, it would be
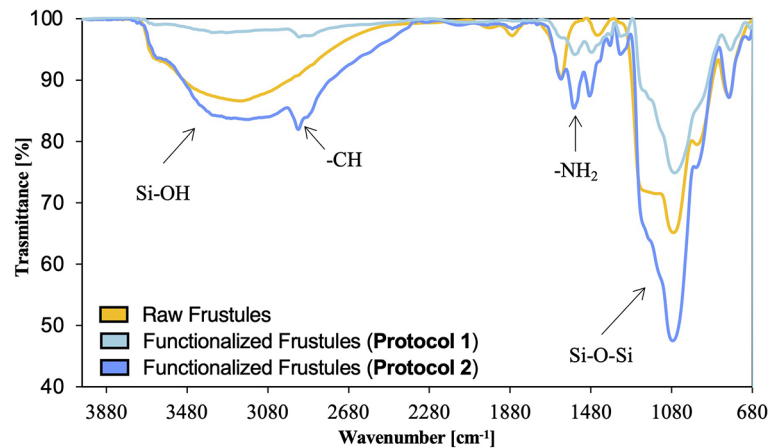
FIGURE 6 | FTIR spectra of raw and functionalized frustules using *Protocol 1* and *Protocol 2*.

highly favourable for removal of heavy metals, as there would be no requirement for pre-treatment of the contaminated, real wastewater pH. FTIR analysis of raw frustules after the adsorption test, showed no significant changes in the FTIR spectrum with respect to that of untreated material. In contrast, the intensity of the -NH$_2$ band of functionalized frustules decreases, indicating the involvement of this functional group in the adsorption process. No significant changes in the spectra were detected at different pH conditions, indicating that the hydrogen ion potential does not imply the degradation of frustule silane coating.

FIGURE 7 | Adsorption of Ni (1.10 mg/L) of functionalized (*Protocol 1* and *Protocol 2*) and raw frustules at three pH conditions after 24-hour treatment. Data are reported as averaged values of triplicates ± standard deviation and analyzed by two-way ANOVA (****p-value < 0.0001).

The rate of Ni removal surely indicates the potential of the functionalized frustules as adsorbent material. After only 10 min, the functionalized frustules removed 97.97% of Ni (from 30 to 0.61 mg/L), whilst the raw frustules removed only 3% (from 30 to 29.12 mg/L) after 5 hours (**Figure 8**).

After centrifugation, at the end of the experiment, the functionalized frustule samples had dark red colour, in contrast with the start of the experiment when both raw and functionalized frustules appeared white. This evidence indicates that the interaction of Ni with -amino and -thiol groups caused the formation of Ni-NH$_2$ and Ni-SH complexes on the surface of modified biosilica (**Figure 9**).

These results suggest that functionalized frustules of *S. pinnata* can be considered as a novel and alternative adsorbent material.

Alternative adsorbents for heavy metal remediation, such as activated carbons, zeolites, clay minerals and nano- materials (Burakov et al., 2018), have their limitations, i.e. the removal efficiency is usually strongly dependent on temperature or pH (Sharma et al., 2007; Priyantha and Bandaranayaka, 2011), they are still for eco-compatibility and toxicity (Lu and Astruc, 2018), and also too costly, limiting their widespread use (Lin et al., 2018). For example, wollastonite, a regularly proposed adsorbent for Ni remediation, has not reached the removal efficiency of functionalized *S. pinnata*. In the present study, with only 0.2 g/L of frustules there was 97.97% Ni removal in 10 min, to obtain the same results with wollastonite around 20 g/L of adsorbent would be required (Sharma et al., 1990). Comparable removal capacities have been reached using alumina nanoparticles removing 96.6% of Ni (0.0255 g/L) after 120 minutes (Sharma et al., 2007), magnetic nanoparticles, are capable of removing 97.6% of Ni (25 mg/L) after 35 min (Gautam et al., 2015), and electrospun nanofiber membranes, can remove 80% of Ni (100 mg/L) after 120 minutes (Aliabadi et al., 2013). However, in comparison with functionalized frustules, production costs of these other adsorbents are high. This being so, there is still a need for further investigations to improve the biosorption process and to offset costs of using functionalized frustules which would
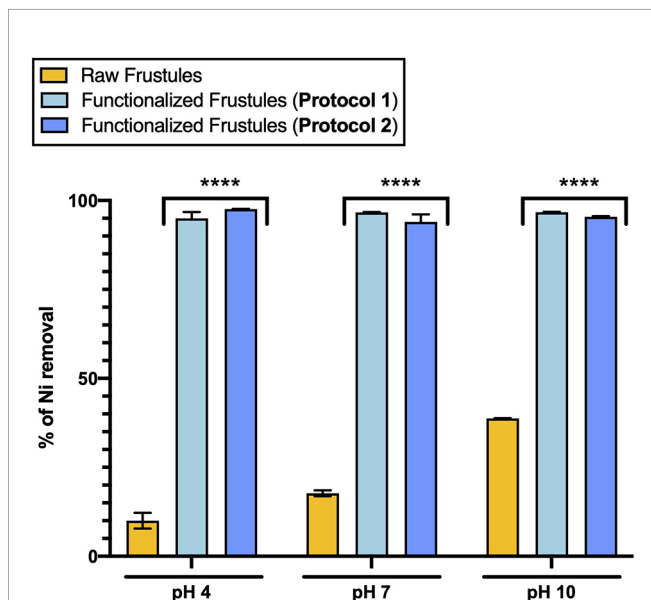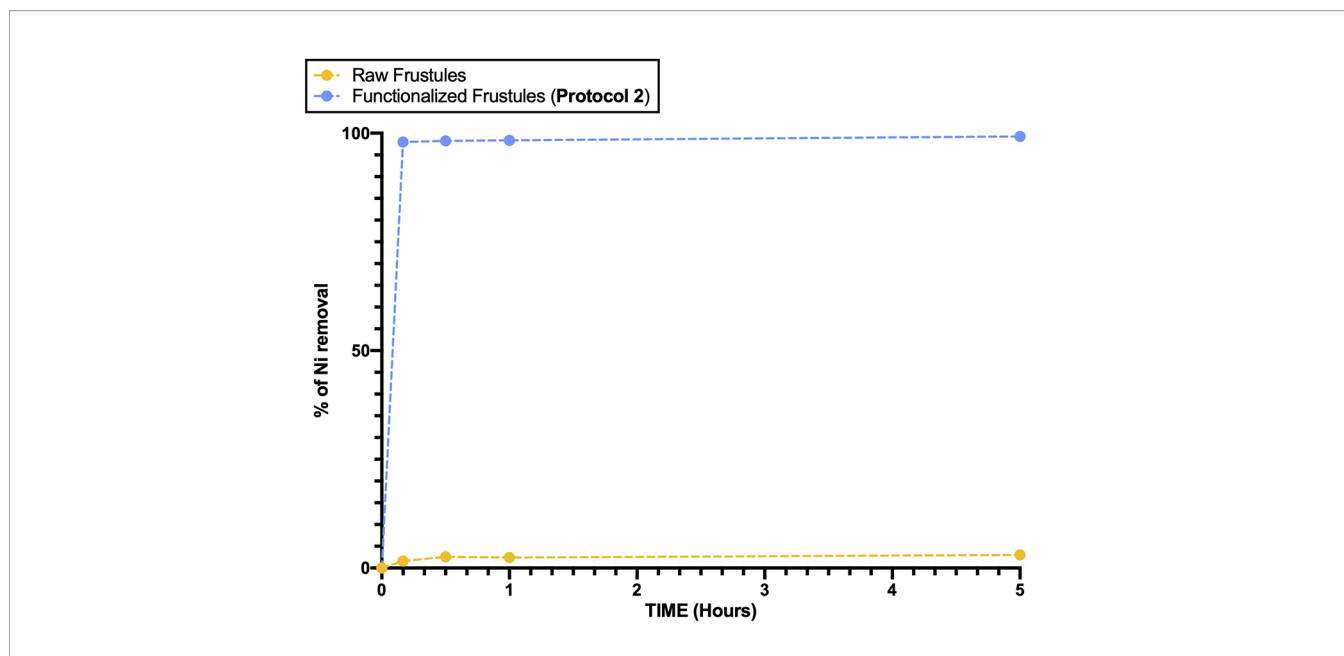
FIGURE 8 | Ni removal efficiency of raw and functionalized frustules as a function of time. Data are reported as averaged values of triplicates ± standard deviation.
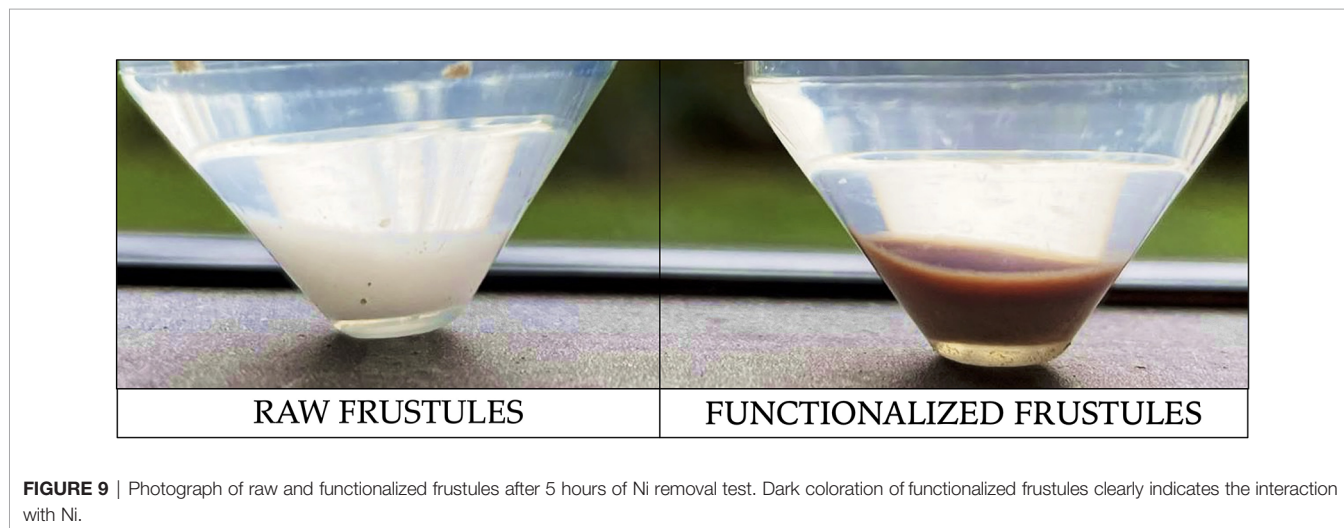

FIGURE 9 | Photograph of raw and functionalized frustules after 5 hours of Ni removal test. Dark coloration of functionalized frustules clearly indicates the interaction with Ni.

include the possibility of regeneration of the biosorbent and the recovery of metals for their potential reuse.

Diatomite, another alternative adsorbent, is much more comparable to the frustules of *S. pinnata* (ElSayed, 2018) as it also has high porosity, large surface area and small particle size. Like *S. pinnata* frustules, raw diatomite, possesses a weak affinity for metal ion binding, and functionalization is also required to enhance their adsorption capacity (Wu et al., 2021). The potential of modified and raw diatomite to remove metals has been widely studied (Khraisheh et al., 2004; Danil de Namor et al., 2012; Kabiri et al., 2015; Nosrati et al., 2017; Zhao et al., 2019; El Ouardi et al., 2020), but there are some inherent problems. The intrinsic heterogeneity of raw diatomite and the

presence of different impurities (such as metal oxides) can influence heavy metals removal potential of diatomite and can make the functionalization process of this material problematic, thus affecting the production of a reproducible adsorbent. In contrast, monospecific mass culture-derived frustules, present a purer and more predictable substrate, allowing for reproducible production that can be easily functionalized.

CONCLUSIONS

The results here reported indicate that functionalized frustules of *S. pinnata* are highly capable of removing Ni from aqueous

solutions. The surface functionalization method here proposed avoids unwanted organosilane polymerization on the material surface, allowing for porous structure retention while granting consistent surface enrichment in specific metal-binding functional groups. The removal efficiency of functionalized frustules of *S. pinnata* is independent from the hydrogen ion concentration, in contrast with other bio-silica based adsorbents that are strongly dependent from pH, limiting their extensive use. In addition, the frustules used in the present study were essentially a by-product of diatom biomass cultivated in a controlled system for other purposes, therefore this approach valorizes the leftover of a diatom biorefinery and improves the economical sustainability for the production at large scale of this adsorbent. Finally, the use of frustules from a single species allows for a predictable and structurally homogeneous nanoporous material, making the functionalization process more reproducible by the development and optimization of an *ad hoc* protocol able to preserve frustule surface features, nanoporous patterns and morphology. The system here presented will be further characterized to determine the maximum Ni concentration removable per unit weight of functionalized frustules and to evaluate the removal capacity toward other metallic species. Different functionalization agents will be also considered to optimize the -NH$_2$ and -SH surface concentration. With further investigations on the recovery and desorption mechanisms of metals and the original functionalized biomass, the possibility to further reduce costs would allow for much larger scale operations. Finally, the expansion of the diatom cultivation process, and the increased drawdown of atmospheric CO$_2$, would certainly improve the ecological sustainability of the whole process.

DATA AVAILABILITY STATEMENT

The original contributions presented in the study are included in the article/supplementary material. Further inquiries can be directed to the corresponding author.

AUTHOR CONTRIBUTIONS

RC and SS contributed to conception and design of the study. SS and NE organized the database. SS and SF performed the statistical analysis. SS, SF, NE, and RC wrote the first draft of the manuscript. SDS, SC, and ADG wrote sections of the manuscript. All authors contributed to manuscript revision, read, and approved the submitted version.

FUNDING

REFERENCES

Aliabadi, M., Irani, M., Ismaeili, J., Piri, H., and Parnian, M. J. (2013). Electrospun Nanofiber Membrane of PEO/Chitosan for the Adsorption of Nickel, Cadmium, Lead and Copper Ions From Aqueous Solution. *Chem. Eng. J.* 220, 237–243. doi: 10.1016/J.CEJ.2013.01.021

Ali, H., Khan, E., and Ilahi, I. (2019). Environmental Chemistry and Ecotoxicology of Hazardous Heavy Metals: Environmental Persistence, Toxicity, and Bioaccumulation. *J. Chem.* 2019. doi: 10.1155/2019/6730305

Anedda, A., Carbonaro, C. M., Clemente, F., Corpino, R., and Ricci, P. C. (2003). Mesoporous Silica Photoluminescence Properties in Samples With Different Pore Size. *Mater. Sci. Eng. C.* 23, 1073–1076. doi: 10.1016/J.MSEC.2003.09.077

Arranz, A., Palacio, C., García-Fresnadillo, D., Orellana, G., Navarro, A., and Muñoz, E. (2008). Influence of Surface Hydroxylation on 3-Aminopropyltriethoxysilane Growth Mode During Chemical Functionalization of GaN Surfaces: An Angle-Resolved X-Ray Photoelectron Spectroscopy Study. *Langmuir* 24, 8667–8671. doi: 10.1021/la801259n

Arrieta, J., Jeanneret, R., Roig, P., and Tuval, I. (2020). On the Fate of Sinking Diatoms: The Transport of Active Buoyancy-Regulating Cells in the Ocean. *Philos. Trans. R. Soc. A.* 378:20190529. doi: 10.1098/RSTA.2019.0529

Bligh, E. G., and Dyer, W. J. (1978). A Rapid Method of Total Lipid Extraction and Purification. *Can. J. Biochem. Physiol.* 37:911–917. doi: 10.1139/o59-099

Burakov, A. E., Galunin, E. V., Burakova, I. V., Kucherova, A. E., Agarwal, S., Tkachev, A. G., et al. (2018). Adsorption of Heavy Metals on Conventional and Nanostructured Materials for Wastewater Treatment Purposes: A Review. *Ecotoxicol. Environ. Saf.* 148, 702–712. doi: 10.1016/J.ECOENV.2017.11.034

Cempel, M., and Nikel, G. (2006). Nickel: A Review of its Sources and Environmental Toxicology. *Polish. J. Environ. Stud.* 15, 375–382.

Danil de Namor, A. F., El Gamouz, A., Frangie, S., Martinez, V., Valiente, L., and Webb, O. A. (2012). Turning the Volume Down on Heavy Metals Using Tuned Diatomite. A Review of Diatomite and Modified Diatomite for the Extraction of Heavy Metals From Water. *J. Hazard. Mater.* 241–242, 14–31. doi: 10.1016/j.jhazmat.2012.09.030

De Angelis, R., Melino, S., Prosposito, P., Casalboni, M., Lamastra, F. R., Nanni, F., et al. (2016). The Diatom *Staurosirella Pinnata* for Photoactive Material Production. *PloS One* 11 (11), e0165571. doi: 10.1371/journal.pone.0165571

De Stefano, M., De Stefano, L., and Congestri, R. (2009). Functional Morphology of Micro- and Nanostructures in Two Distinct Diatom Frustules. *Superlattices. Microstruct.* 46, 64–68. doi: 10.1016/j.spmi.2008.12.007

De Tommasi, E., Congestri, R., Dardano, P., De Luca, A. C., Managò, S., Rea, I., et al. (2018). UV-Shielding and Wavelength Conversion by Centric Diatom Nanopatterned Frustules. *Sci. Rep.* 81 (8), 1–14. doi: 10.1038/s41598-018-34651-w

Di Caprio, G., Coppola, G., Stefano, L., De Stefano, M., De Antonucci, A., Congestri, R., et al. (2014). Shedding Light on Diatom Photonics by Means of Digital Holography. *J. Biophotonics* 7, 341–350. doi: 10.1002/jbio.201200198

El Ouardi, Y., Branger, C., Toufik, H., Laatikainen, K., Ouammou, A., and Lenoble, V. (2020). An Insight of Enhanced Natural Material (Calcined Diatomite) Efficiency in Nickel and Silver Retention: Application to Natural Effluents. *Environ. Technol. Innov.* 18, 100768. doi: 10.1016/j.eti.2020.100768

ElSayed, E. S. E. B. (2018). Natural Diatomite as an Effective Adsorbent for Heavy Metals in Water and Wastewater Treatment (A Batch Study). *Water Sci.* 32, 32–43. doi: 10.1016/J.WSJ.2018.02.001

Ferrara, M. A., Dardano, P., De Stefano, L., Rea, I., Coppola, G., Rendina, I., et al. (2014). Optical Properties of Diatom Nanostructured Biosilica in Arachnoidiscus Sp: Micro-Optics From Mother Nature. *PloS One* 9 (7), e103750. doi: 10.1371/journal.pone.0103750

FreshWater Information System for Europe (WISE) (2018). "European Waters," in *Assessment of Status and Pressures* (Luxembourg: Publications Office of the European Union). EEA Report No 7/2018. doi: 10.2800/303664

Gautam, R. K., Gautam, P. K., Banerjee, S., Soni, S., Singh, S. K., and Chattopadhyaya, M. C. (2015). Removal of Ni(II) by Magnetic Nanoparticles. *J. Mol. Liq.* 204, 60–69. doi: 10.1016/J.MOLLIQ.2015.01.038

Gilbert-López, B., Barranco, A., Herrero, M., Cifuentes, A., and Ibáñez, E. (2017). Development of New Green Processes for the Recovery of Bioactives From *Phaeodactylum Tricornutum*. *Food Res. Int.* 99, 1056–1065. doi: 10.1016/j.foodres.2016.04.022

González-Fortuna, G., Arteaga-Larios, N., Nahmad, Y., Navarro-Contreras, H. R., and García-Meza, J. V. (2021). Frustules of *Amphora* Sp. As a Photonic Crystal With Photoluminescent CdS Nanoparticles. *Luminescence* 36, 788–794. doi: 10.1002/BIO.4003

Gutiérrez Moreno, J. J., Pan, K., Wang, Y., and Li, W. (2020). Computational Study of APTES Surface Functionalization of Diatom-Like Amorphous SiO2 Surfaces for Heavy Metal Adsorption. *Langmuir* 36, 5680–5689. doi: 10.1021/acs.langmuir.9b03755

Hamm, C. E., Merkel, R., Springer, O., Jurkojc, P., Maiert, C., Prechtelt, K., et al. (2003). Architecture and Material Properties of Diatom Shells Provide Effective Mechanical Protection. *Nature* 421, 841–843. doi: 10.1038/nature01416

Haworth, E. Y. (2007). A Scanning Electron Microscope Study of Some Different Frustule Forms of the Genus *Fragilaria* Found in Scottish Late-Glacial Sediments *British Phycol.* 10 (1), 73–80. doi: 10.1080/00071617500650071

Heintze, C., Formanek, P., Pohl, D., Hauptstein, J., Rellinghaus, B., and Kröger, N. (2020). An Intimate View Into the Silica Deposition Vesicles of Diatoms. *BMC Mater.* 2, 1–15. doi: 10.1186/S42833-020-00017-8

Jakša, G., Štefane, B., and Kovač, J. (2014). Influence of Different Solvents on the Morphology of APTMS-Modified Silicon Surfaces. *Appl. Surf. Sci.* 315, 516–522. doi: 10.1016/J.APSUSC.2014.05.157

Kabiri, S., Tran, D. N. H., Azari, S., and Losic, D. (2015). Graphene-Diatom Silica Aerogels for Efficient Temoval of Mercury Ions From Water. *ACS Appl. Mater. Interfaces* 22, 11815–11823. doi: 10.1021/acsami.5b01159

Khraisheh, M. A. M., Al-degs, Y. S., and Mcminn, W. A. M. (2004). Remediation of Wastewater Containing Heavy Metals Using Raw and Modified Diatomite. *Chem. Eng. J.* 99, 177–184. doi: 10.1016/J.CEJ.2003.11.029

Kiran Marella, T., Saxena, A., and Tiwari, A. (2020). Diatom Mediated Heavy Metal Remediation: A Review. *Bioresour. Technol.* 305, 123068. doi: 10.1016/j.biortech.2020.123068

Lamastra, F. R., De Angelis, R., Antonucci, A., Salvatori, D., Prosposito, P., Casalboni, M., et al. (2014). Polymer Composite Random Lasers Based on Diatom Frustules as Scatterers. *RSC. Adv* 4, 61809. doi: 10.1039/c4ra12519c

Legambiente. (2020). *H2O, La Chimica Che Inquina L'acqua*. Available at: https://www.legambiente.it/rapporti/h%e2%82%82o-la-chimica-che-inquina-lacqua/.

Lin, Q., Liu, E., Zhang, E., Nath, B., Shen, J., Yuan, H., et al. (2018). Reconstruction of Atmospheric Trace Metals Pollution in Southwest China Using Sediments From a Large and Deep Alpine Lake: Historical Trends, Sources and Sediment Focusing. *Sci. Total. Environ.* 613–614, 331–341. doi: 10.1016/J.SCITOTENV.2017.09.073

Liu, X., Hu, Q., Fang, Z., Zhang, X., and Zhang, B. (2009). Magnetic Chitosan Nanocomposites: A Useful Recyclable Tool for Heavy Metal Ion Removal. *Langmuir* 25, 3–8. doi: 10.1021/LA802754T

Lu, F., and Astruc, D. (2018). Nanomaterials for Removal of Toxic Elements From Water. *Coord. Chem. Rev.* 356, 147–164. doi: 10.1016/J.CCR.2017.11.003

Mack, J. B. C., Gipson, J. D., Du Bois, J., and Sigman, M. S. (2017). Ruthenium-Catalyzed C–H Hydroxylation in Aqueous Acid Enables Selective Functionalization of Amine Derivatives. *J. Am. Chem. Soc.* 139 (28), 9503–9506. doi: 10.1021/jacs.7b05469

Mitchell, J. G., Seuront, L., Doubell, M. J., Losic, D., Voelcker, N. H., Seymour, J., et al. (2013). The Role of Diatom Nanostructures in Biasing Diffusion to Improve Uptake in a Patchy Nutrient Environment. *PloS One* 8 (5), e59548. doi: 10.1371/journal.pone.0059548

Nosrati, A., Larsson, M., Lindén, J. B., Zihao, Z., Addai-Mensah, J., and Nydén, M. (2017). Polyethyleneimine Functionalized Mesoporous Diatomite Particles for Selective Copper Recovery From Aqueous Media. *Int. J. Miner. Process.* 166, 29–36. doi: 10.1016/j.minpro.2017.07.001

Novelli, F., De Santis, S., Punzi, P., Giordano, C., Scipioni, A., and Masci, G. (2017). Self-Assembly and Drug Release Study of Linear L,D-Oligopeptide-Poly(Ethylene Glycol) Conjugates. *N. Biotechnol.* 37, 99–107. doi: 10.1016/J.NBT.2016.07.005

Ogata, K., Koike, K., Sasa, S., Inoue, M., and Yano, M. (2009). X-Ray Photoelectron Spectroscopy Characterization of Aminosilane Anchored to ZnO Nanorod Arrays Grown by an Aqueous Solution Method With Microwave-Assisted Heating. *J. Vac. Sci. Technol. B. Microelectron. Nanom. Struct. Process. Meas. Phenom.* 27, 1834. doi: 10.1116/1.3155824

Parikh, A. N., Allara, D. L., Azouz, I. B., and Rondelez, F. (2002). An Intrinsic Relationship Between Molecular Structure in Self-Assembled N-Alkylsiloxane Monolayers and Deposition Temperature. *J. Phys. Chem.* 98, 7577–7590. doi: 10.1021/J100082A031

Priyantha, N., and Bandaranayaka, A. (2011). Interaction of Cr(VI) Species With Thermally Treated Brick Clay. *Environ. Sci. Pollut. Res.* 18, 75–81. doi: 10.1007/S11356-010-0358-3/FIGURES/7

Rea, I., Martucci, N. M., De Stefano, L., Ruggiero, I., Terracciano, M., Dardano, P., et al. (2014). Diatomite Biosilica Nanocarriers for siRNA Transport Inside Cancer Cells. *Biochim. Biophys. Acta - Gen. Subj.* 1840, 3393–3403. doi: 10.1016/j.bbagen.2014.09.009

Rogato, A., and De Tommasi, E. (2020). Physical, Chemical, and Genetic Techniques for Diatom Frustule Modification: Applications in Nanotechnology. *Appl. Sci.* 10, 8738. doi: 10.3390/APP10238738

Savio, S., Congestri, R., and Rodolfo, C. (2021). Are We Out of the Infancy of Microalgae-Based Drug Discovery? *Algal. Res.* 54, 102173. doi: 10.1016/j.algal.2020.102173

Savio, S., Farrotti, S., Paris, D., Arnaìz, E., Díaz, I., Bolado, S., et al. (2020). Value-Added Co-Products From Biomass of the Diatoms *Staurosirella Pinnata* and *Phaeodactylum Tricornutum*. *Algal. Res* 47, 101830. doi: 10.1016/j.algal.2020.101830

Selvaraj, V., Thomas, N., Anthuvan, A. J., Nagamony, P., and Chinnuswamy, V. (2018). Amine-Functionalized Diatom Frustules: A Platform for Specific and Sensitive Detection of Nitroaromatic Explosive Derivative. *Environ. Sci. Pollut. Res.* 25, 20540–20549. doi: 10.1007/s11356-017-0916-z

Sharma, Y. C., Gupta, G. S., Prasad, G., and Rupainwar, D. C. (1990). Use of Wollastonite in the Removal of Ni(II) From Aqueous Solutions. *Water. Air. Soil Pollut.* 49, 69–79. doi: 10.1007/BF00279511

Sharma, Y. C., Prasad, G., and Rupainwar, D. C. (2007). Removal of Ni(II) From Aqueous Solutions by Sorption 37, 183–191. doi: 10.1080/00207239108710629

Solomons, N. W., Viteri, F., Shuler, T. R., and Nielsen, F. H. (1982). Bioavailability of Nickel in Man: Effects of Foods and Chemically-Defined Dietary Constituents on the Absorption of Inorganic Nickel. *J. Nutr.* 112, 39–50. doi: 10.1093/jn/112.1.39

Terracciano, M., De Stefano, L., Santos, H. A., Lamberti, A., Martucci, N. M., Shahbazi, M. A., et al. (2015). "Diatomite Nanoparticles as Potential Drug Delivery Systems," in *3rd IEEE International Conference on BioPhotonics, BioPhotonics 2015*, 1–3. doi: 10.1109/BioPhotonics.2015.7304032

Townley, H. E. (2011). "Diatom Frustules: Physical, Optical, and Biotechnological Applications," in *The Diatom World. Cellular Origin, Life in Extreme Habitats and Astrobiology*, eds. Seckbach, J., and Kociolek, P. (Springer Science +Business Media) 19, 273–289. doi: 10.1007/978-94-007-1327-7_12

Tozak, K. Ö., Erzengin, M., Sargin, I., and Ünlü, N. (2013). Sorption of DNA by Diatomite-Zn(II) Embedded Supermacroporous Monolithic p(HEMA) Cryogels. *EXCLI J.* 12:670–680.

Uthappa, U. T., Sriram, G., Jung, H.-Y., Yu, J., Brahmkhatri, V., Sriram, G., et al. (2018). Nature Engineered Diatom Biosilica as Drug Delivery Systems. *Artic. J. Control. Release* 281, 70–83. doi: 10.1016/j.jconrel.2018.05.013

Wang, J. K., and Seibert, M. (2017). Prospects for Commercial Production of Diatoms. *Biotechnol. Biofuels.* 10, 16. doi: 10.1186/s13068-017-0699-y

Water Framework Directive (2000). Official Journal of the European Communities, L327/1. *Directive 2000/60/EC of the European Parliament and of the Council; Establishing a Framework for Community Action in the Field of Water Policy*, L327/1.

World Health Organisation (2005). "Nickel in Drinking-Water," in *Background Document for Development of WHO Guidelines for Drinking-Water Quality*. (Geneva: World Health Organization). (WHO/HEP/ECH/WSH/2021.6). Licence: CC BY-NC-SA 3.0 IGO.

Wu, S., Wang, C., Jin, Y., Zhou, G., Zhang, L., Yu, P., et al. (2021). Green Synthesis of Reusable Super-Paramagnetic Diatomite for Aqueous Nickel (II) Removal. *J. Colloid. Interface Sci.* 582, 1179–1190. doi: 10.1016/J.JCIS.2020.08.119

Yu, Y., Addai-Mensah, J., and Losic, D. (2012). Functionalized Diatom Silica Microparticles for Removal of Mercury Ions. *Sci. Technol. Adv. Mater.* 13, 15008–15019. doi: 10.1088/1468-6996/13/1/015008

Zhang, Y., Ding, T., Zhang, Z., Xu, L., and Zhang, Q. (2015). Enhanced Adsorption of Trivalent Arsenic From Water by Functionalized Diatom Silica Shells. *PloS One* 10, e0123395. doi: 10.1371/JOURNAL.PONE.0123395

Zhao, Y., Tian, G., Duan, X., Liang, X., Meng, J., and Liang, J. (2019). Environmental Applications of Diatomite Minerals in Removing Heavy

Metals From Water. *Ind. Eng. Chem. Res.* 58, 11638–11652. doi: 10.1021/acs.iecr.9b01941